Li *et al. Cancer Nanotechnology* (2022) 13:21
https://doi.org/10.1186/s12645-022-00127-w

Cancer Nanotechnology

RESEARCH Open Access

Nanomicelles co-loaded with doxorubicin and salvianolic acid A for breast cancer chemotherapy

Zhiyong Li[1,2†], Jiali Liu[1†], Zheng Sun[1], Yanli Li[1,3], Bin Yu[1], Feng Zhao[1], Hongbo Wang[1*] and Hui Xu[1*]

†Zhiyong Li and Jiali Liu contributed equally to this work

*Correspondence: hongbowang@ytu.edu.cn; xuhui@ytu.edu.cn

[1] School of Pharmacy, Collaborative Innovation Center of Advanced Drug Delivery System and Biotech Drugs in Universities of Shandong, Key Laboratory of Molecular Pharmacology and Drug Evaluation (Yantai University), Ministry of Education, Yantai University, No. 32 Qingquan Road, Yantai 264005, People's Republic of China
[2] Guangdong Zhongrun Pharmaceutical R&D Co., Ltd., Guangzhou 510623, China
[3] Department of Pharmaceutics, Binzhou Hospital of Traditional Chinese Medicine, Binzhou 256601, China

Abstract

Background: Multi-drug delivery system based on polymer carrier is emerging for alleviating dose-limiting toxicities of first-line cytotoxic anticancer drugs, such as doxorubicin (DOX) for breast cancer chemotherapy. By co-loading the premium natural antioxidant salvianolic acid A (SAA) through colloidal self-assembly of amphiphilic copolymer, we herein developed CPMSD, a complex polymeric micellar system to overcome cardiotoxicity associated with DOX.

Results: Optimal formulation was obtained by DOE study and CPMSD micelles were well constructed by using mPEG-PCL for entrapment at a drug–carrier mass ratio of 1:5 and DOX–SAA mass ratio of 1:4. Molecular dynamics simulation revealed the ratiometrical co-encapsulation of SAA into the hydrophobic cavity but DOX to ball-shaped surface of micelles due to hydrophilicity. Characterization study manifested favorable biopharmaceutical properties, such as small and uniform particle size, fairly high drug loading capacity, as well as good colloidal stability and controlled drug release. CPMSD maintained anticancer efficacy of DOX and the action mechanism, which did not be affected by co-administering SAA. More to the point, it was of great benefit to systemic safety and cardioprotective effect against oxidative stress injuries associated with DOX in tumor-bearing mice.

Conclusions: All the findings substantiated that CPMSD would be a promising multifunctional nanosystem of DOX for breast cancer chemotherapy.

Keywords: Multifunctional nanomicelles, Doxorubicin, Salvianolic acid A, Breast cancer chemotherapy, Cardioprotection

Introduction

Breast cancer is among the most frequently diagnosed cancer and now becomes the leading cause of cancer death in women worldwide (Bray et al. 2018). According to the latest data from the International Agency for Research on Cancer (IARC) of the World Health Organization (WHO), more than 2.26 million new cases of breast cancer were diagnosed in 2020, which were responsible for 11.7% of all new cases of cancer. So far, chemotherapy remains an essential treatment for preventing recurrence in many patients with stage I–III breast cancer. Given the relatively unfavorable prognosis,

it is even the sole systemic therapy with demonstrated efficacy for triple-negative breast cancer (TNBC), and only chemotherapeutic agents are approved by the Food and Drug Administration (FDA) (Waks and Winer 2019).

The anthracycline antibiotic doxorubicin (DOX, Fig. 1) is one of the most effective chemotherapeutic agents approved for various cancers, which is also most commonly used in standard regimens, such as AC4, AC-T, and TaxAC for breast cancer. Specifically, the use of DOX appears most important in patients with more lymph node involvement and with TNBC disease (Blum et al. 2017). Overall, chemotherapy regimens containing both DOX and taxane achieve the greatest risk reduction and remain the appropriate choice in high-risk patients (Bray et al. 2018). However, the clinical application of DOX is usually associated with multiple adverse effects, particularly the cardiac mortality that may affect ~11% of the patients under treatment (Chatterjee et al. 2010). More to the point, DOX-related cardiotoxicity is typically a kind of dose-limiting toxicity, leading to limited cumulative tolerable dose and lowered therapeutic efficacy. It has been demonstrated that even 26% of patients develop congestive heart failure at a cumulative dose of 550 mg/m^2 of DOX (Ewer and Ewer 2010). Therefore, the DOX therapies with attenuated toxicity but maintained anticancer efficacy are still a great challenge.

Over the past decades, much research has been devoted to investigating solution ways against DOX-induced cardiotoxicity, mainly including development of new drug delivery systems and discovery of efficient cardioprotective adjuvants. The PEGylated liposomal doxorubicin (Doxil) is a liposome-encapsulated form of DOX available in the market with reduced cardiotoxicity and an improved pharmacokinetic profile. Major limitations of this improved DOX formulation are complicated preparation process and high cost, although several clinical trials have demonstrated that its monotherapy is an effective alternative to other commonly used chemotherapy regimens in patients with metastatic breast cancer (Duggan and Keating 2011). Meanwhile, various cardiac protective agents have been evaluated, including dexrazoxane, the only one approved by FDA for treatment of anthracycline extravasation (Cvetković and Scott 2005; Kane et al. 2008). Unfortunately, its clinical use has been restricted due to carcinogenic potential

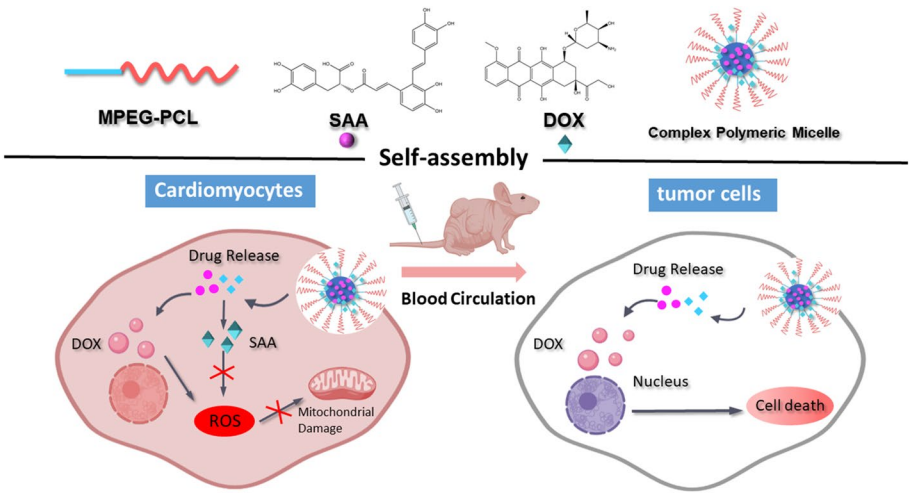

Fig. 1 Schematic representation of the self-assembly of CPMSD and its multifunction for cancer therapy

with an increased risk for development of acute myeloid leukemia and myelodysplastic syndrome (Shaikh et al. 2016; Spalatoceruso et al. 2019). In recently years, oxidative stress caused by excessive production of reactive oxygen species (ROS) has been the most widely investigated and accepted mechanism of DOX-induced cardiotoxicity, and natural antioxidative molecules with good efficacy and safety have attracted increasingly high attention (Mitry and Edwards 2016; Kaiserova et al. 2007; Sun et al. 2017; Benzer et al. 2018; Guo et al. 2018). However, drug delivery system research is still a huge challenge to realize further development and clinical application of these promising cardioprotective candidates mainly due to undesirable physico-chemical properties.

Nanofabrication by self-assembly provides polymeric micelles (PMs) a typical core–shell structure, which solubilizes and stabilizes hydrophobic molecule in the core, while the hydrophilic shell can improve the steric stabilization by reducing opsonization and prolong blood circulation (Torchilin 2007; Gong et al. 2013; Wicki et al. 2015). With the advantages of adequate function and easy manufacture, PMs are becoming more and more attractive in drug delivery, especially for co-delivering conventional cytotoxic agent and some medical adjuvant to produce distinctive effect of killing two birds with one stone (Yu et al. 2020; Kuerban et al. 2020; Zhang et al. 2018).

MPEG-PCL diblock copolymer is a common carrier material for nanomicelles and also a research hotspot in recent years. Poly(ε-caprolactone) (PCL) has good biodegradable and biocompatible which is an ideally suitable for long-term drug delivery due to its slow degradation, which has good application prospects in anticancer drugs and other drug carriers (Sinha et al. 2004). Although there are no drugs with mPEG-PCL as carrier yet on the market, a large number of preclinical studies have proved its superiority (Kwon and Kataoka 2012). Some researchers used mPEG-PCL to encapsulate poorly soluble drugs, such as cyclosporine A, paclitaxel, and curcumin to make nanomicelles. Compared with free drugs, micelles can effectively increase the circulation time of drugs in the blood and improve their bioavailability in vivo (Wei et al. 2018; Zhai et al. 2017). The application of mPEG-PCL polymer provides more options for the treatment of breast cancer.

Much recent research has demonstrated that salvianolic acid A (SAA), an active polyphenol from *Salvia miltiorrhiza*, is a potent natural antioxidant with great benefit against various oxidative stress injuries, such as DOX-induced cardiotoxicity. Recently, it has been approved in China for oral administration for the treatment of diabetic peripheral neuropathy, and angina attack and acute myocardial infarction, respectively (Lin et al. 1992; Fan et al. 2012, 2015; Hou et al. 2017). As illustrated in Fig. 1, the present study just aimed to develop a complex nanomicellar formulation (CPMSD) that dually loaded DOX and SAA to produce multiple beneficial effects for breast cancer chemotherapy. By using biocompatible copolymer as drug carrier, the novel formulation of CPMSD provided an efficient way co-delivering SAA with DOX for injection, also overcome the major limitations of its unsatisfactory physico-chemical properties, such as instability, poor solubility, and low systemic bioavailability (Zhou et al. 2013; Shen et al. 2009; Xu et al. 2014). Herein, the multifunctional nanomicellar system of CPMSD was fabricated under the optimal formulation to meet the demands of clinical application, and both the therapeutic efficacy and mechanism of action were investigated via in vitro and in vivo models. To the best of our knowledge, so far there have been no reports

about complex nano-formulation co-delivering DOX and SAA. There is no doubt that the resulting multifunctional nanomicellar system of CPMSD would pay the way for breast cancer chemotherapy with DOX-containing regimens.

Material and methods

Materials

Doxorubicin hydrochloride (DOX) was supplied by Beijing Ouhe Technology Co., Ltd (Beijing, China), and salvianolic acid A (SAA) was purchased from Nanjing Guangrun Biotechnology Co., Ltd. (Nanjing, China), respectively. The macroinitiator used was polyethylene ethylene glycol monomethyl ether (mPEG) with a number-average molecular weight of 2000 obtained from Sigma-Aldrich Co (St Louis, MO, USA), and all the amphiphilic diblock copolymers were synthesized in our laboratory by ring-opening polymerization according to the method previously reported (Liu et al. 2015). All solvents and other reagents were available commercially and of analytical grade or higher. Ultra-pure water prepared by a lab purification system was used throughout the experiment.

Cells and animals

The MCF-7 human breast adenocarcinoma cell line was acquired from Chinese Academy of Science Cell Bank for Type Culture Collection (Shanghai, China), and the MCF-10A non-cancerous human breast epithelial cell line was donated by the Affiliated Hospital of Binzhou Medical College (Yantai, China). DMEM containing 10% fetal bovine serum and 1% penicillin/streptomycin (HyClone Laboratories, Logan, USA) was used for cell culture in a humidified incubator with 5% CO_2 at 37 °C. The female athymic nude mice (BALB/c, nu/nu) with body weight of 20 ± 2 g (aging from 6 to 8 weeks) were obtained from Shanghai Experimental Animal Center (Shanghai, China). All animal experimental procedures were conducted by following the National Institutes of Health (NIH) guidelines and approved by the Animal Experimentation Ethics Committee of Yantai University, China.

Preparation of CPMSD and characterization

By using amphiphilic diblock copolymer as drug carrier, the nanomicelles co-encapsulating DOX and SAA (CPMSD) were prepared via a simple and reliable thin-film hydration method as previously reported (Zhang et al. 2018). In brief, a specified amount of copolymer and SAA were firstly dissolved in acetone at first. After 5 min of stirring, the solvent was slowly evaporated under water bath at 45 ± 2 °C to form a thin-layer film, dissolved with physiological saline at 45 °C to obtain a transparent micelle solution, followed by successive addition of the phosphate-buffered solution (PBS; 10×, pH 7.4) and DOX aqueous solution. The mixture was stirred at room temperature (~ 20 min), filtered through a 0.22-μm filter, and then subjected to lyophilization under vacuum (FD-1C-80 freeze dryer, Shanghai, China) to obtain the freeze-dried powder of CPMSD stored at − 20 °C until use (See Additional file 1: Table S1 and Figure S2).

The micelles were reconstituted to obtain an aqueous solution (~ 1 mg/mL) for morphology observation by using transmission electron microscopy (JEM-1400 TEM, JEOL, Tokyo, Japan). The mean diameter and particle size distribution were measured by dynamic light scattering method (Zetasizer Nano ZS 90, Malvern, UK) at room

temperature with a scattering angle of 90°, and the polydispersity index (PDI) was calculated to evaluate size distribution.

HPLC–UV quantification of both drugs was performed simultaneously via a Waters e2695 HPLC system. The chromatographic separation was conducted on a TC-C18 column (250 mm × 4.6 mm i.d., 5 μm; Agilent Technologies) at 30 °C, and the injection volume was 10 μL. The mobile phase composed of methanol and 0.2% formic acid (55:45) was delivered at a flow rate of 1 mL/min. The detection wavelength was set at 254 nm, and the retention time was 6.16 min for DOX and 9.63 min for SAA, respectively. For determination of drug loading content (DLC) and entrapment efficiency (EE), the lyophilized powder of micelles was weighed (M), reconstituted to obtain an aqueous solution (~ 1 mg/mL); then about tenfolds of methanol was added for demulsification, followed by vortex mixing (5 min) and filtration (0.22 μm, Millipore); the filtrate then was subject to HPLC analysis for determination of the amount of drugs (M1). Meanwhile, the same aliquot of the aqueous solution of micelles was subject to centrifugation (8000 rpm × 10 min) to remove free drugs; then the supernatant was processed using the same program as above for HPLC assay of the amount of drug loaded in micelles (M2). DLC and EE then were calculated according to the ratio of M1 to M, and M2 to M1, respectively. The in vitro drug release was investigated by a dialysis method as reported previously (Liu et al. 2015; Zhang et al. 2022). Briefly, total DOX concentration was set at 0.2 mg/mL, and the PBS solution containing 1% polysorbate 80 (pH 7.4) was used as release medium for incubation at 37 °C. At pre-set intervals, the sample outside dialysis bag with a molecular weight cut-off of 8–10 kDa (Shanghai Yuanye Biotechnology Co., Ltd., China) was withdrawn and mixed with mobile phase for HPLC analysis to determine the amount of drug release for calculation of in vitro drug release rate.

Formula optimization

Design of experiment (DOE) was performed for formula optimization of CPMSD via Box–Behnken design (BBD) method due to the high efficiency with small numbers of tests (Jiang et al. 2014). Design-Expert® (Version 8.0.6, State-Ease Inc., Minneapolis, MN, USA) was applied for a three-factor-three-level BBD, which included the major independent variables, such as polymer type (X_1), mass ratio of DOX to SAA (X_2), and drug feed ratio (X_3) as displayed in Table 1. The dependent variables were particle size (Y_1), drug loading (Y_2), and entrapment efficiency (Y_3), and the design matrix containing a total of 17 experimental runs was obtained as shown in Table 2.

Table 1 Independent variables and levels involved in Box–Behnken design

Independent variable	Level		
	Low (− 1)	Medium (0)	High (+ 1)
X_1 types of polymer	mPEG-PLA	mPEG-PCL	mPEG-PCL-Phe(Boc)
X_2 mass ratio of DOX/SAA	1:2	1:4	1:6
X_3 feed ratio	4:1	5:1	8:1

Table 2 Box–Behnken experimental design and the observed responses

Run	Independent variable			Dependent variable		
	X_1	X_2	X_3	Y_1 (nm)	Y_2 (%)[a]	Y_3 (%)[b]
1	0	0	0	17.11 ± 1.30	13.3 ± 0.4	85.6 ± 4.8 (79.1 ± 3.8, 92.0 ± 4.0)
2	0	−1	−1	18.78 ± 0.75	14.5 ± 1.0	75.0 ± 2.1 (67.5 ± 2.9, 82.4 ± 2.3)
3	0	+1	+1	17.65 ± 0.97	4.5 ± 0.6	43.0 ± 2.0 (37.1 ± 1.3, 45.5 ± 5.2)
4	0	0	0	16.99 ± 1.12	13.4 ± 1.1	92.9 ± 3.3 (87.0 ± 2.5, 98.7 ± 2.8)
5	0	0	0	16.98 ± 0.90	13.9 ± 1.5	100.4 ± 4.2 (97.1 ± 5.3, 103.6 ± 1.8)
6	0	−1	+1	17.66 ± 2.11	8.0 ± 0.7	80.6 ± 5.2 (74.9 ± 4.3, 90.4 ± 7.1)
7	0	0	0	16.82 ± 2.01	15.1 ± 1.0	101.6 ± 15.0 (101.2 ± 12.2, 102.3 ± 12.6)
8	+1	+1	0	17.16 ± 1.01	16.5 ± 1.2	101.8 ± 2.8 (99.9 ± 3.3, 103.8 ± 1.4)
9	−1	−1	0	224.5 ± 22.34	11.7 ± 0.7	87.8 ± 4.6 (81.6 ± 3.2, 93.9 ± 4.2)
10	−1	0	+1	15.03 ± 1.67	9.9 ± 0.6	78.9 ± 6.7 (72.5 ± 5.1, 85.3 ± 5.9)
11	0	+1	−1	16.77 ± 0.52	19.8 ± 1.5	96.1 ± 8.7 (89.7 ± 7.1, 102.5 ± 7.0)
12	+1	0	−1	18.44 ± 0.73	16.6 ± 1.7	87.7 ± 5.3 (81.1 ± 4.5, 94.2 ± 4.1)
13	+1	−1	0	266.9 ± 24.21	11.7 ± 0.7	72.7 ± 6.5 (66.6 ± 5.7, 78.9 ± 4.9)
14	+1	0	+1	18.23 ± 1.31	10.6 ± 0.5	93.9 ± 8.0 (87.5 ± 6.2, 100.2 ± 6.1)
15	0	0	0	17.46 ± 0.63	15.7 ± 1.2	91.6 ± 11.3 (85.2 ± 9.2, 98.1 ± 9.3)
16	−1	+1	0	16.06 ± 0.37	15.0 ± 1.4	84.9 ± 7.8 (78.8 ± 6.0, 90.9 ± 6.8)
17	−1	0	−1	115.5 ± 9.78	14.6 ± 0.9	61.7 ± 9.1 (55.9 ± 7.8, 67.5 ± 7.1)

[a] The data are the sum of DOX and SAA

[b] The data are the mean of two drugs and the EE value of separate drug is presented successively in brackets for DOX and SAA

Molecular dynamics simulation

Molecular dynamics simulation was performed to investigate the molecular mechanism of drug entrapment into micelles by using the open source HyperChem software (Professional 80, Hypercube Inc., Gainesville, USA). At first, the 3-D structure of copolymer or small-molecule drug was theoretically simulated by means of molecular mechanics (MM) and molecular dynamics (MD) (Zhang et al. 2018). According to the initial structure, a series of geometrical optimization then were performed at MM level via OPLS method by using the steepest descent algorithm until the root mean square gradient was less than 0.10 kcal/(mol·Angstrom). After heating from 0 to 600 K, the optimized structure then was subject to a series of MD simulations running at 600 K with each runtime of 100 ps to obtain a lower energy minimum, for which the CHARMM27 force field was used and the solvent effect was considered implicitly (Jorgensen et al. 1996; Yin et al. 2021; Foloppe and MacKerell 2000). Finally, random docking was performed to examine the interactions among drug and copolymer based on the optimal 3-D structures of copolymer and small-molecule drug (DOX or SAA).

Assessment of in vitro cytotoxicity and cell uptake

The in vitro cytotoxicity against MCF-7 or MCF-10A cells was evaluated by using the Cell Counting Kit-8 (CCK-8, Dalian Meilun Biotech Co., Ltd, China). Briefly, the cells in logarithmic growth phase were prepared as single-cell suspensions, and seeded into 96-well plates at a density of 4×10^3 per well for pre-incubation overnight. Then the cells were subjected to different treatment paradigms for 24 h incubation. Drug was aspirated

and PBS (pH 7.4) was used to rinse cells thrice; then cell viability assessment was performed according to the kit manual by recording the absorbance of medium with CCK-8 (10%, v/v) after 6 h incubation via a microplate reader at 450 nm (Li et al. 2020a). All the results were the average measurement of six replicate wells and are expressed as mean ± SD.

For cell uptake studies, the MCF-7 cell line was inoculated on a glass petri dish (35 mm × 12 mm, 1×10^5 cells/mL) for 24 h. After removal of the spent medium, fresh DMEM medium containing drug at an equivalent DOX concentration of 0.2 μM was placed and cells were incubated for 2 h. Then the medium was aspirated, and the cells were rinsed thrice with PBS (pH 7.4) and then put in 4% paraformaldehyde fix solution for 15 min. After discarded the fix liquid, cells were rinsed thrice with PBS. After operated procedures above, the cells were further incubated in DAPI solution for 15 min. After removal of the dye, cells were rinsed thrice with PBS and subjected to observation under a confocal laser scanning microscopy (CLSM).

In vivo studies using a murine xenograft model

The xenograft tumor model in nude mice was established by subcutaneously inoculating human breast cancer MCF-7 cells (4×10^7 cells) (Zuo et al. 2019); the tumor-bearing mice with the volume of solid tumors reached 170–200 mm^3 then were randomized into four groups ($n = 8$), and i.v. administered once every 2 days for repeated 5 times with various formulations, namely, CPMSD micelles, free DOX solution, the cocktail solution of free DOX and SAA, or the vehicle as a negative control. For each administration, normal saline was used as a vehicle and the dosage was 2.5 mg/kg for DOX and 10 mg/kg for SAA equivalent (Zhang et al. 2018). At 24 h after the last dosing, blood samples were collected to prepare serum for further biochemical estimations; then all the mice were sacrificed and tumors and major tissues were immediately harvested, weighed, and stored for further analysis.

Quantitation, data analysis, and statistics

Drug content of both drugs in micelles was determined by a dual wavelength HPLC method using Waters e2695 HPLC system. Briefly, The chromatographic separation was performed on a TC-C18 column (250 mm × 4.6 mm, 5 μm) at 30 °C via isocratic elution with the mixture of methanol and 0.2% aqueous formic acid (55/45, v/v) at a flow rate of 1.0 mL/min, and the detection wavelength was set at 420 nm during 0–12 min for DOX, and 254 nm during 12–25 min for SAA, respectively. UPLC-MS/MS assay was performed to determine drug content in biosamples, such as plasma and tissues by using an AB Sciex Triple Quad™ 4500 system connected with Shimadzu LC-30AD via electrospray ionization (ESI) interface. The mass spectrometer was operated in positive mode by using multiple reaction monitoring (MRM) of the transitions *m/z* 544.2/396.8 for DOX and *m/z* 749.4/591.5 for the internal standard azithromycin, while in negative mode using the transitions *m/z* 493.2/294.9 for SAA and *m/z* 367.0/149.0 for the internal standard curcumin, respectively.

Colorimetric assays were performed by using commercial kits to evaluate major markers of cardiotoxicity, such as lactate dehydrogenase (LDH), creatine kinase (CK) and cardiac troponin T (cTnT) in serum, and malondialdehyde (MDA) and superoxide

dismutase (SOD) in cardiac tissue. For histological examination, the paraffin-embedded sections of the left half heart of mice were sliced (5 μm) and then HE staining for light microscope observations was performed. All specimens were analyzed, and the representative images were captured by two pathologists with blind investigation.

All data are presented as mean ± standard deviation (SD) of replicate measurements. Student's *t*-test was applied to statistical analysis of experimental data by using the statistical software package SPSS 20.0 (International Business Machines Corporation, New York, USA). Statistical significance was indicated by $p < 0.05$ and more statistical significance by $p < 0.01$.

Results and discussion

Optimal formulation of CPMSD based on DOE

Taking into consideration the fact that Box–Behnken design (BBD) method has been widely applied in DOE due to the high efficiency with small numbers of tests (Jiang et al. 2014), a 3-factor-3-level BBD was performed herein for optimizing the formulation of CPMSD. As shown in Table 1, the independent variables were some crucial factors concerned with complex polymeric micelles fabrication, such as the types of polymer (X_1), mass ratio of DOX to SAA (X_2), and the feed ratio of carrier to drugs (X_3), for which the corresponding levels were set according to preliminary one-factor tests for screening. More to the point, three common used amphiphilic block copolymers were applied for micellar formula optimization, namely, mPEG-PLA, mPEG-PCL, and mPEG-PCL-Phe (Boc), wherein the hydrophilic segment was mPEG with an average molecular weight of about 2000, and the hydrophobic segment was selected from polylactide (PLA), polycaprolactone (PCL), or that capped with *N*-*t*-butoxycarbonyl-phenylalanine (Boc-Phe). All these copolymers were synthesized and characterized in our lab, and the drug entrapment properties had been well demonstrated in previous studies (Zhang et al. 2018; Liu et al. 2015; Jiang et al. 2014). Resultantly, the design matrix containing a total of 17 experimental runs was obtained from BBD as shown in Table 2, which contained 12 factorial points at the midpoint of edge for each process space, and 5 replicates at the center point for estimation of pure error sum of squares. Each experimental run then could be performed in light of the design matrix in random order to avoid bias.

It is well known that the dimensional characteristics of nanomicelles may contribute to passive targeting to tumor through the enhanced permeability and retention (EPR) effect, since it preferred to avoid macrophages uptake and clearance by mononuclear phagocyte system (MPS) or the reticuloendothelial system (RES), and achieved long circulation and fairly high chance of reaching tumor site. Furthermore, the nanomicelles with high DLC and EE but small particle size are usually expected to avoid immune clearance and maintain desired systematic bioavailability (Li et al. 2020b). Herein, several key performance indices (KPI) of micellar system thus were used as the dependent variables for statistical analysis and evaluation of CPMSD formulation, namely, particle size (Y_1), drug loading capacity (DLC, Y_2), and entrapment efficiency (EE, Y_3).

The observed responses of KPI (Table 2) clearly revealed that there was significant differentiation among these experimental runs. Specifically, the particle size ranged from 15 to 267 nm, while DLC and EE changed between 4.5 and 19.8%, and 43.0% and 101.8%, respectively. The influence of all these independent variables (X_1, X_2, X_3) on KPI was

further investigated by using multiple regression analysis. The cubic polynomial regression model for each KPI could be obtained with determination coefficient (R^2) more than 0.9 and the p-value less than 0.05, and the 3-D response surface plots illustrated overall influence of the independent variables (Fig. 2A–C). Among all the three formulation factors involved in the present study, X_3, namely, the feed ratio of copolymer carrier to both drugs, was found to be the most important one for fabricating CPMSD micelles, especially had a great impact on DLC and EE. According to these results, all the three factors X_1, X_2, and X_3 thus were determined at the medium level for fabricating CPMSD micelles. That is to say, the multifunctional nanomicelles of CPMSD could be achieved by using the amphiphilic block copolymer of mPEG-PCL as a carrier for encapsulating both drugs under a carrier–drug mass ratio of 5:1 and DOX–SAA mass ratio of 1:4.

On the basis of optimal formulation obtained from BBD study, several batches of CPMSD nanomicelles were prepared by conventional thin-film hydration technique, then characterized for verification (Zhang et al. 2018). DLS assay clearly demonstrated that the CPMSD micelles were usually the uniform and small particles with mean particle size ranging within 15 to 25 nm and the PDI values less than 0.2. Meanwhile, HPLC quantitation indicated that the DLC values for DOX and SAA together were (15.7 ± 0.8)%, and EE values were generally more than 95%. All these KPI values determined were in close agreement with the predicted values of optimal micellar system of CPMSD from DOE model that showed particle size of 17.1 nm, DLC of 14.3%, and EE of 94.4%, suggesting that the DOE-based optimal formulation would be reliable for fabricating the aimed dual drug-loaded nanomicelles of CPMSD for further evaluation.

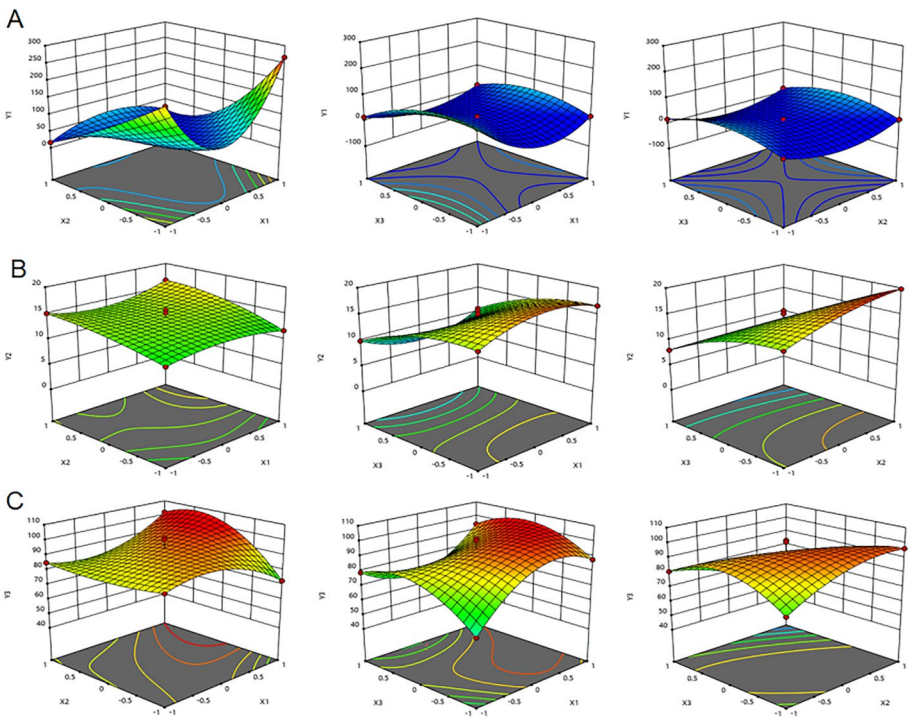

Fig. 2 Response surface plots of DOE showing the effects of formulation on **A** particle size, **B** drug loading capacity and **C** entrapment efficiency of CPMSD

Molecular mechanism of drugs entrapment into micelles

The possible mechanism of amphiphilic block copolymer encapsulating both drugs to form novel nanomicelles of CPMSD was further investigated in the present study. The approaches of molecular mechanics (MM) and molecular dynamics (MD) were applied to examine molecular interactions among the polymeric carrier (mPEG-PCL) and small-molecule drug (DOX and SAA) based on simulating their theoretical structures (Jorgensen et al. 1996; Foloppe and MacKerell 2000). As illustrated in Fig. 3a–d, the copolymer initially displayed a curvilinear conformation, then gradually bended and changed with the heating process, and finally formed into a spherical shape after 100 ps MD simulation, which consisted of hydrophilic and hydrophobic parts and provided suitable binding sites for small molecules. Meanwhile, both small-molecule drugs constantly adjusted the conformation and distance from copolymer to obtain favorable interaction modes (Fig. 3e–h). Resultantly, the copolymer encapsulated SAA into the hydrophobic cavity and DOX to the hydrophilic surface, respectively (Fig. 3i).

Chemically DOX is a kind of antibiotics with the amino sugar linked to anthracycline via a glycosidic bond (Fig. 1), which contributes to its hydrophilicity and the preference for binding to the hydrophilic surface of the copolymer mPEG-PCL. In contrast, SAA is a kind of salvianolic acid with fairly high hydrophobicity, thus could tight bind with the hydrophobic cavity of the copolymer. More to the point, the phenolic hydroxyl and carboxyl groups in SAA (Fig. 1) would significantly enhance the molecular interaction with the other drug molecule DOX via its basic amino sugar. From this point of view, SAA plays an important role as a bridge between DOX and the copolymer, which greatly promotes copolymer–drug interaction, and leads to significant increase in drug encapsulation efficiency of the complex micellar system CPMSD, especially for the relatively hydrophilic drug molecule DOX. The findings from MD simulation clearly demonstrated that CPMSD could act as a new and efficient dual drug-loaded micellar DDS by

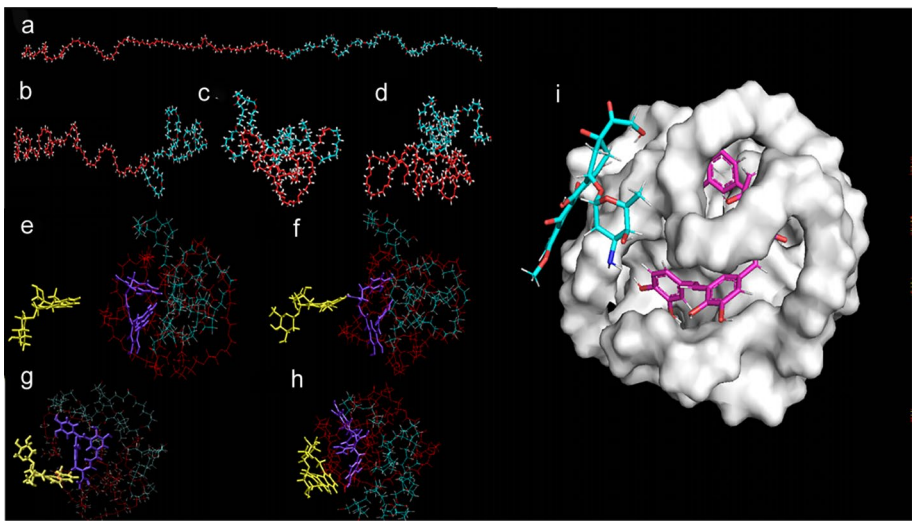

Fig. 3 Molecular dynamics simulation of drug entrapment into CPMSD. **a**–**d** MD simulation process of the copolymer (mPEG-PCL); **e**–**h** merging copolymer with drugs (DOX and SAA), DOX—yellow stick, SAA—purple stick; **i** the final 3-D map of copolymer–drug interaction (copolymer—gray solid surface, DOX—blue stick, SAA—pink stick)

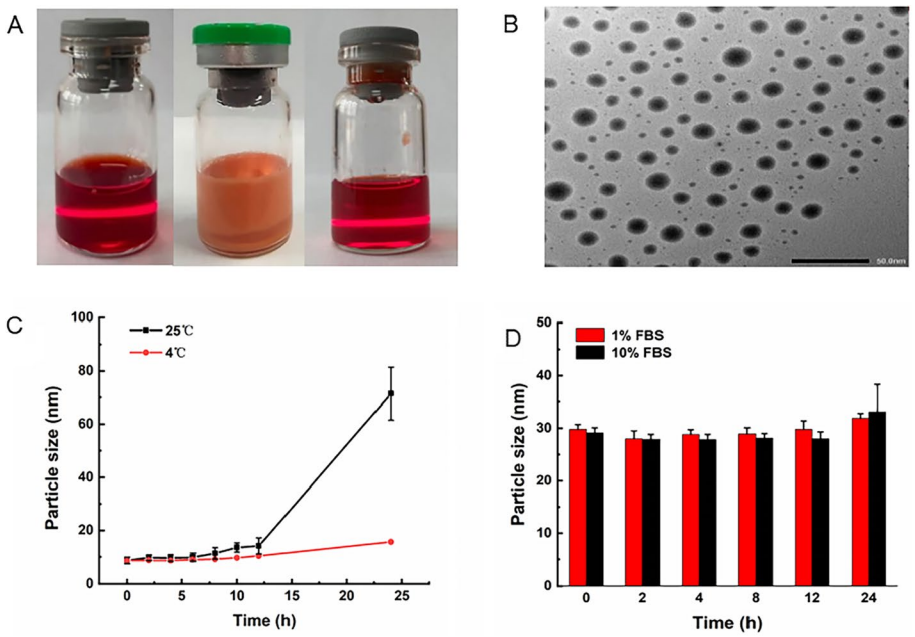

Fig. 4 Characterization of CPMSD by **A** appearance observation (→ solution before lyophilization, lyophilized powder, solution after lyophilization), **B** TEM imaging (×150,000), **C** effect of temperature on particle size, and **D** stability of particle size in the incubation system containing FBS at 37 °C ($n = 3$)

Table 3 Effect of lyophilization and storage temperature on the stability of CPMSD ($n = 3$)

Parameters	Lyophilization		Storage[a]			
	Before	After	4 °C 1 week	25 °C 1 week	4 °C 1 month	25 °C 1 month
Particle size (nm)	21.6 ± 1.5	20.2 ± 2.6	21.9 ± 1.7	21.2 ± 1.0	22.6 ± 2.1	23.8 ± 2.3
DLC (%)	16.1 ± 0.6	16.2 ± 0.8	16.2 ± 1.2	16.8 ± 1.2	15.9 ± 1.9	16.4 ± 0.4
EE (%)	99.6 ± 3.4	97.7 ± 2.8	96.8 ± 4.0	95.2 ± 3.1	96.9 ± 3.9	96.2 ± 2.1

[a] The data are collected from the lyophilized powders of CPMSD

a unique mechanism involved in drug entrapment, which might also result in specific drug release profiles of CPMSD.

Colloidal properties and stability of CPMSD

Polymeric nanomicelles are a kind of self-assembled colloidal particles for drug delivery, and the colloidal stability has a great impact on pharmaceutical performance, such as in vitro and in vivo drug release behaviors (Moore et al. 2015). Herein, an overall investigation was performed on the colloidal properties and stability of CPMSD, as well as the influence of technique process and ambient conditions. Resultantly, the freeze–drying process provided a yellowish red lyophilized powder of CPMSD micelles with good disparity but no collapse or atrophy, and the micellar solutions before and after lyophilization were both observed as a stable colloidal suspension with typical Tyndall effect (Fig. 4A). Meanwhile, the micelles before and after lyophilization showed no significant difference in these performance indices, such as particle size, DLC, and EE (Table 3).

The findings thus demonstrated that the freeze–drying process would not alter major physico-chemical properties of the present micellar system of CPMSD. The TEM image for morphology further revealed that CPMSD micelles were uniform nanoparticles with spherical or nearly spherical shape and a typical particle size of about 20 nm (Fig. 4B).

In order to get a better understanding of the influence of temperature on colloidal stability of CPMSD, six batches of fresh prepared micellar solution (2 mL/branch) were divided into two groups ($n = 3$) and placed at 4 °C and room temperature (25 °C), respectively; then the particle size was monitored periodically. Resultantly, it was found that the micellar solution freshly prepared could maintain a stable particle size at 4 °C for at least 24 h, and a significant increase in particle size was observed after storage at room temperature for 12 h (Fig. 4C), suggesting that the CPMSD micelles should be made into lyophilized powders for long-term storage. The long-term stability of CPMSD lyophilized powders at various temperatures then was studied according to the major parameters of micelles, such as particle size, DLC, and EE. As shown in Table 3, there was no significant difference of any parameter between the lyophilized powder freshly prepared and that after storage ($p > 0.05$). The results provided further evidence for the good stability of CPMSD, which could keep stable as lyophilized powders stored at 4 °C or room temperature for at least 1 month.

The particle size change in simulated serum was further inspected to evaluate the colloidal stability of CPMSD in systemic circulation. The micelles were incubated with fetal bovine serum (FBS, pH 7.4) at 37 °C under gentle stirring, and an aliquot of the sample was withdrawn for the measurement according to the time schedule. As shown in Fig. 4D, there was no significant change with time in micellar particle size within 24 h incubation in the simulated body fluid containing 1% or 10% FBS ($p > 0.05$), indicating a good colloidal stability of CPMSD in vivo. Meanwhile, the CPMSD micellar particles in PBS displayed a slightly negative zeta potential, i.e., (1.77 ± 0.49) mV, and this value became more negative with increasing FBS content, namely (3.20 ± 0.53) mV and (3.62 ± 0.27) mV in the incubation system containing 1% FBS and 10% FBS, respectively. These findings together demonstrated the coating effect of endogenous proteins, such as serum albumin, might be chiefly responsible for in vivo colloidal stability of CPMSD.

In vitro drug release from CPMSD

The in vitro drug release characteristics of CPMSD were investigated via dialysis method, and PBS solution containing 1% Tween 80 (pH 7.4) was used as the release medium to maintain the chemical stability and sink condition for both DOX and SAA. Resultantly, there was significant difference in the in vitro release profile between DOX and SAA (Fig. 5).

Although the encapsulated drugs were both sustained released from CPMSD, DOX had a much higher release rate at early stage than SAA did, and an initial release burst with a percent cumulative release of 45% within 0.5 h could be observed. The drug release of DOX increased steadily, and the cumulative drug release amount reached a peak of about 90% within 3 h. In contrast, the nanomicelles of CPMSD constantly released SAA at a rather slow rate, which had a percent cumulative release up to 70% within 72 h.

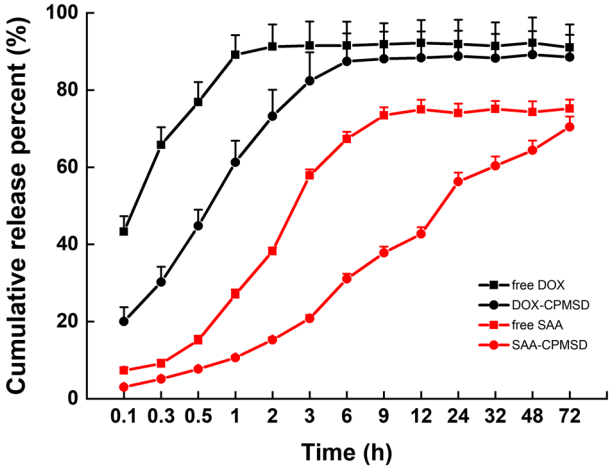

Fig. 5 The in vitro drug release profile in PBS (pH 7.4) at 37 °C ($n = 3$)

Table 4 Model fitting for in vitro drug release from nanomicelles of CPMSD micelles

Model	DOX[a]	SAA[a]
Zero-order equation	$Y = 0.78t + 71.07$ (0.2103)	$Y = 0.86t + 21.50$ (0.7811)
First-order equation	$Y = 87.66\,[1 - \exp(-1.26t)]$ (0.9819)	$Y = 65.18\,[1 - \exp(-0.10t)]$ (0.9765)
Higuchi equation	$Y = 6.36t^{1/2} + 61.67$ (0.4924)	$Y = 8.55t^{1/2} + 7.05$ (0.9402)

[a] The data in parenthesis are the determination coefficient for model fitting

Furthermore, the kinetic mechanism of drug release from CPMSD was investigated by fitting several common kinetic models to the cumulative release profiles, including the zero-order, first-order, and Higuchi models. As shown in Table 4, the first-order model was determined as the optimal one with the highest goodness of fit, and the values of determination coefficient (R^2) reached up to 0.97 for both drugs. Thus, it could be concluded that non-constant diffusion was the chief mechanism involved in drug release from CPMSD micelles for both DOX and SAA, while matrix swelling and dissolution could be negligible in the present dual drug-loaded polymeric micellar system. All these findings clearly demonstrated the special drug releasing characteristics of CPMSD and also provided a strong evidence for the above-mentioned distinctive mechanism of drug entrapment based on MD studies, which thought that CPMSD micelles would be prone to a relatively fast drug release for DOX from the hydrophilic surface, but an extended release for SAA from the inner core.

In vitro cytotoxicity and cellular uptake

Taking into account the fact that DOX is a cytotoxic drug, herein the in vitro cytotoxicity was investigated by using CCK-8 assay of cell viability. For the sake of comparison, the non-cancerous human breast epithelial cell line MCF-10A was used along with the human breast cancer cell line MCF-7, and various treatments related to the present micellar system of CPMSD were involved, including free solution of DOX or SAA, and the cocktail formulation of DOX and SAA. It was found that free DOX alone could significantly inhibit in vitro proliferation of both cell lines in a

similar concentration-dependent manner (Fig. 6A), and the half inhibitory concentration (IC_{50}) was determined as 0.27 μM for MCF-7 cells, and 0.56 μM for MCF-10A cells, respectively. These findings were in good consistence with those reported previously and clearly demonstrated the potent cytotoxicity of DOX toward normal cells, although it is indeed an effective chemotherapy agent for human breast cancer (Tsou et al. 2015). However, the case was quite different for SAA. As shown in Fig. 6B, free drug of SAA alone at a final concentration within 10 μM had almost no significant influence on the in vitro proliferation of MCF-7 or MCF-10A cells, and the relative inhibition rate was not more than 20%, indicating that SAA is not the same kind of cytotoxic agent as DOX. The result was in line with the findings concerning

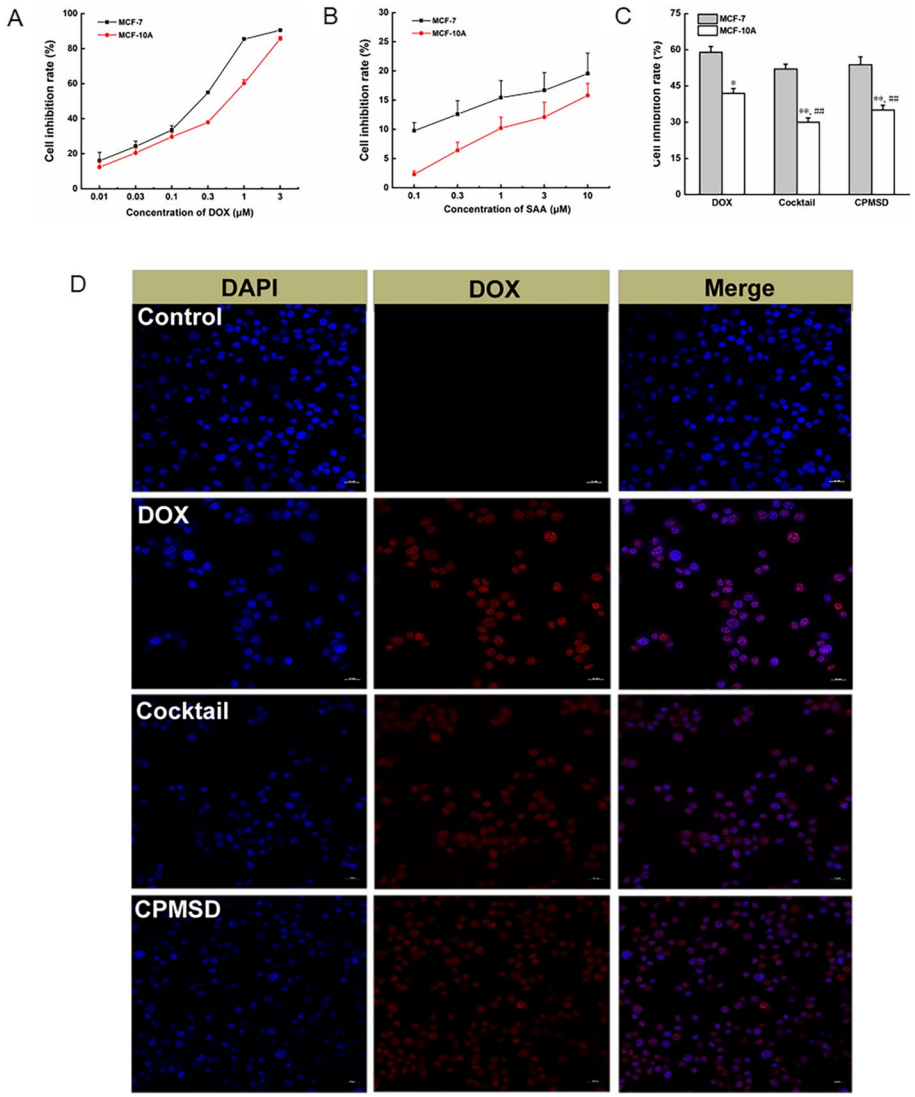

Fig. 6 Evaluation of anticancer characteristics against in vitro proliferation of MCF-7 cells. **A** Dose–response relationship of free DOX (mean ± SD, $n = 6$). **B** Comparison of antiproliferative effect of the preparations related with CPMSD at an equivalent final concentration of 230 ng/mL for DOX, and 920 ng/mL for SAA, respectively (mean ± SD, $n = 6$; $^{*}p < 0.05$ compared with DOX in MCF-7, $^{\#}p < 0.05$ compared with DOX in MCF-10A). **C** CLSM observation (×40 objective) of cellular uptake

biological and pharmacological activities of this natural product reported previously (Lin et al. 1992; Fan et al. 2012, 2015; Hou et al. 2017; Zhou et al. 2013) and suggested that SAA–DOX combination may be a promising comprehensive treatment strategy for breast cancer through different mechanisms of action from the two drugs.

Then the influence of SAA on in vitro cytotoxicity of DOX was studied under various conditions. As shown in Fig. 6C, free DOX alone at a final concentration of 230 ng/mL caused a relative inhibition rate of about 60% against MCF-7 and ~45% against MCF-10A cell line, respectively, which were significantly different ($p < 0.05$) and indicated that breast cancer cells may be more sensitive to the cytotoxic agent DOX than normal mammary epithelial cells. When compared with free DOX alone at the same concentration (230 ng/mL), the combination treatment of CPMSD or cocktail preparation at a same weight ratio of DOX to SAA (1:4) displayed similar inhibitory potency against breast cancer MCF-7 cells, and no significance difference was observed among the three groups ($p > 0.05$). It is worth noting that the case was totally different for the effect on MCF-10A cells. The combination of SAA exhibited obvious protection on the normal mammary epithelial cells via cocktail or CPMSD preparation, and the inhibition rate could be significantly reduced in contrast to free DOX alone ($p < 0.05$). More to the point, it was found that CPMSD had a slightly higher inhibition rate against MCF-10A cells than the cocktail of free DOX and SAA, which may be closely related to the slow releasing profile of SAA from CPMSD micelles as mentioned above (Fig. 5). All these findings together, therefore, demonstrated that DOX could be the major active pharmaceutical ingredient responsible for anticancer efficacy of the present micellar system of CPMSD, and the combination with SAA would have not affect anticancer potency of DOX, but lead to beneficial protection against side effect of DOX, such as the cytotoxicity to normal cells.

DOX is an anthracycline drug widely used in breast cancer chemotherapy. So far, the best-known and widely accepted mechanisms are based on the inhibition of DNA replication, transcription, and repair processes, which is mediated by the drug intercalation into DNA and occur in the nucleus (Szaflarski et al. 2013). The final target location of DOX is the nucleus, which is usually regarded as the main target responsible for the anticancer potency of DOX (Li et al. 2019). The cellular uptake of DOX and the effect of CPMSD formulation thus were investigated following the evaluation of anticancer potency in vitro. Cell nuclei were stained by DAPI, and CLSM was employed for observation through detecting its blue fluorescence and the obvious specific red fluorescence of DOX. Continuous increase in the fluorescence intensity of DOX could be clearly observed with extension of the incubation time. After a 2-h incubation, all the three groups treated with DOX at an equivalent concentration displayed similarly strong red fluorescence when compared with the control group without any drug treatment. According to the Merge column, the regions with red fluorescence of DOX were well overlapped with those with blue fluorescence of DAPI and there was no significant difference among these DOX-containing treatments (Fig. 6C), indicating a rapid uptake of DOX almost entirely into the nuclei of MCF-7 cells, no matter what the preparation of DOX was. The results from in vitro evaluation together revealed that the CPMSD preparation might be an efficient nano-formulation of DOX with full maintenance of the anticancer potency and the final target of this chemotherapy drug.

In vivo anticancer efficacy

Female BALB/c nude mice bearing human breast cancer MCF-7 cells were employed to evaluate in vivo therapeutic responses of the CPMSD preparation, such as anticancer efficacy, as well as the protective effect against DOX-induced cardiotoxicity. All the model mice were randomly divided into several groups ($n=8$) administering different formulations of DOX under the same regime, and the antitumor therapeutic efficacy was assessed through characterizing the tumor with time after administration. More specifically, the aim drug DOX, which was delivered by the free drug alone, CPMSD, or the cocktail formulation both with a DOX/SAA mass ratio of 1:4, was intravenously administered at a single DOX dose of 2.5 mg/kg for five times every each other day (Zhang et al. 2018). The mice only given the same volume of vehicle (saline) were used as the negative control (NC) for comparison.

In contrast to the mice in NC group, the animals administered DOX all had drastic inhibition of tumor growth, no matter what the drug formulation was. As illustrated in Fig. 7A, tumor grew gradually in the NC group and the relative tumor volume reached 150% after the last injection of saline, whereas the other three groups (DOX, cocktail, and CPMSD) similarly showed an opposite temporal profile and all displayed a significant difference from the NC group in the relative tumor volume ($p<0.01$). After the accomplishment of all the five DOX dosages, the relative tumor volume was observed ranging from less than 40% to about 50%, which varied with the formulations of DOX. Moreover, significant difference among these DOX formulations could be found after the second dosage, and some tumors were even completely eradicated through treatment by the CPMSD micelles. Since it would take time for the micelles to penetrate into tumors, concentrate at the tumor site, and release drug (Zuo et al. 2019), these findings thus indicated that CPMSD might be a kind of sustained release preparation of DOX with tumor-targeting efficiency, as well as the most potent DOX formulation against breast cancer growth in mice.

In order to confirm the observation of tumor volume changes, all the mice were sacrificed one day after the last dosage and tumors were resected and weighed. As shown in Fig. 7B, the tumor weight averaged 70.1 ± 11.5 mg for the mice in NC group, 25.9 ± 5.6 mg for DOX group, 30.5 ± 7.2 mg for cocktail group, and 27.4 ± 8.7 mg for CPMSD group, respectively. The mice only treated by saline showed the maximum

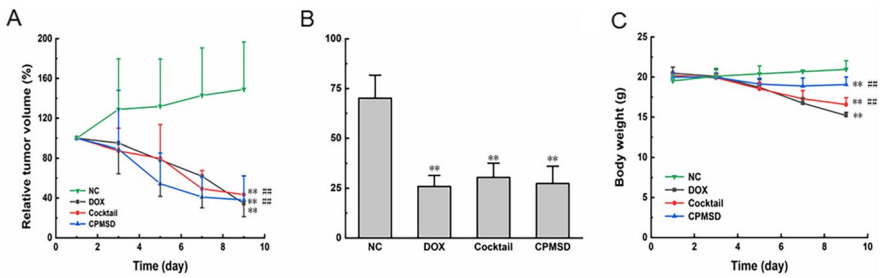

Fig. 7 Evaluation of anticancer efficacy of various preparations in nude mice bearing human breast cancer MCF-7 cells ($n=8$, mean ± SD) by relative tumor volume (**A**), tumor weight (**B**), and body weight change with time (**C**). In each group, the dosage was 2.5 mg/kg for DOX and 10.0 mg/kg for SAA equivalent. *NC* normal saline, *Cocktail* solution of free DOX and SAA, *CPMSD* compound micelles of DOX and SAA, *DOX group* free DOX solution. $^{**}p<0.01$ compared with the NC group and $^{\#\#}p<0.01$ compared with DOX group

mean tumor weight, while all the DOX-containing treatments, no matter what the drug formulation was, led to dramatic shrinkage of the tumor weight in comparison with that in the NC group ($p < 0.01$). Then the tumor growth inhibition (TGI) was calculated to quantify treatment effects. The TGI value for antitumor activity rating reached up to 63.0% by free DOX alone, 56.5% by the cocktail formulation of DOX, and 60.9% by CPMSD preparation, respectively, and there was no significant difference among these DOX formulations ($p > 0.05$).

Meanwhile, the body weight was monitored for each animal to investigate the potential difference in systemic toxicity among various treatments. Although the mice in each group had a similar mean body weight till the second dosage, significant difference could be observed among the three DOX formulations involved after finishing all the five dosages ($p < 0.01$), and the final body weight of the mice in CPMSD group was the closest to that in NC group (Fig. 7C), suggesting excellent biosafety of this DOX formulation. Together with the above-mentioned findings from evaluation of the in vitro cytotoxicity, thus it was concluded that the present dual drug-loaded polymeric micellar system of CPMSD could greatly alleviate systemic toxicity of DOX but not attenuate its in vivo antitumor potency via co-treatment with SAA. As shown in Fig. 8, there were also significant differences in biodistribution profile of both drugs between CPMSD and the simple cocktail formulation of free DOX and SAA. More to the point, the mice administered with CPMSD micelles had the higher amount of SAA in cardiac tissue (Fig. 8B), which would be more beneficial to the cardiac protection against DOX than the simple cocktail formulation. The drug releasing profile of CPMSD together with the metabolic fate of SAA may be responsible for such drug biodistribution characteristics. SAA is known as a kind of natural polyphenol compound with fast and extensive metabolism, leading to a short retention time and very low systemic bioavailability (< 1%) (Hou et al. 2007; Pei et al. 2008). Fortunately, drug encapsulation into CPMSD micelles significantly retarded in vivo metabolic transformation of SAA (unpublished data) and improved the distribution of prototype drug into normal tissues, such as the major target organ of DOX-induced cardiotoxicity, suggesting a possible mechanism for high antitumor potency and low toxicity of the present micellar system of CPMSD.

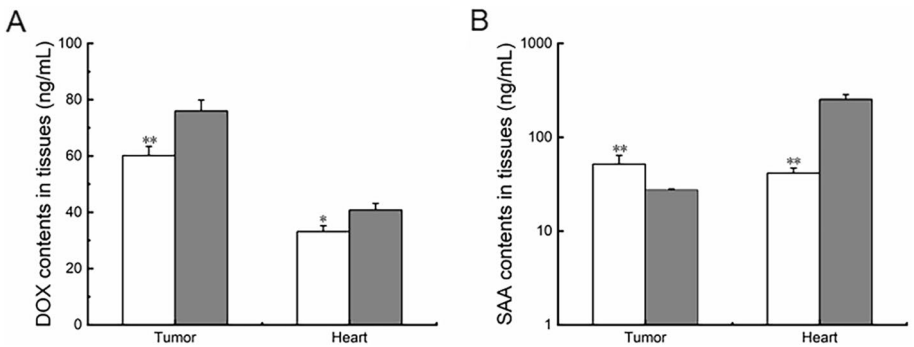

Fig. 8 Drugs content in tumor and heart after administrated CPMSD (gray bar) and cocktail (white bar). $^{**}p < 0.01$ and $^{*}p < 0.05$ compared with CPMSD

In vivo protective effects against cardiotoxicity

The clinical use of DOX is limited by severe cardiotoxic side effects, although it is a potent anticancer drug. Oxidative stress is generally recognized as one of the main mechanisms responsible for DOX-induced cardiotoxicity and much research has recently been devoted to this challenge, mainly including some doxorubicin-antioxidant co-drugs (Chegaev et al. 2013), and dual drug-loaded nano-platform for targeted cancer therapy toward clinical therapeutic efficacy of multifunctionality (Ma et al. 2020). Our present study aimed at the CPMSD formulation for breast cancer chemotherapy, which was a high-performance multifunctional polymeric micellar delivery system co-loading the anticancer drug DOX and the highly potent natural antioxidant SAA. Following evaluation of antitumor efficacy, the detoxification effect of SAA delivered by CPMSD was further investigated in tumor-bearing nude mice through assay of several principal physiological and biochemical markers related to myocardial function, as well as inspection of myocardial histologic changes concerned with cardiotoxicity.

Along with monitoring body weight changes, the heart weight of each animal was measured for calculating the cardiac weight index (CWI) by its ratio to body weight. As shown in Fig. 9A, the NC group had a maximum CWI value of $(0.48 \pm 0.01)\%$, while the minimum value was found as $(0.34 \pm 0.03)\%$ for the mice administered free DOX alone. Significant difference in CWI could be observed between the NC group and any of the other two groups treated with DOX-containing formulation but CPMSD at an equivalent dosage ($p < 0.01$). There was no significant difference between the DOX and cocktail group, even though it was co-administered with the antioxidant agent SAA through the cocktail formulation. However, the CWI value for the mice administered CPMSD micelles was found as $(0.46 \pm 0.02)\%$, which was significantly higher than the other two DOX-containing groups ($p < 0.01$), and even close to that in the NC group ($p > 0.05$). Taking into consideration of the changes in both CWI and body weight (Fig. 7C), these

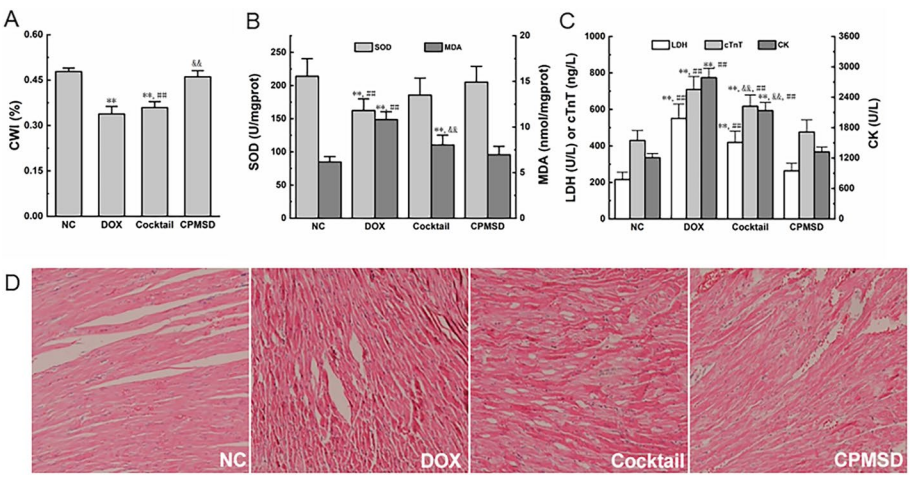

Fig. 9 Evaluation of cardiotoxic effects in nude mice bearing MCF-7 cancer cells by **A** heart weight index, **B** LDH, CK, and cTnT in serum, **C** SOD, MDA in heart tissues ($^{**}p < 0.01$ and $^{*}p < 0.05$, compared with NC, $^{\#\#}p < 0.01$ and $^{\#}p < 0.05$, compared with CPMSD, $^{\&\&}p < 0.01$ and $^{\&}p < 0.05$, compared with DOX), and **D** light microscope observation (×400) of pathological change in mice left ventricles (with the black arrows indicating representative morphological changes, such as cell necrosis, superficial cytoplasm, and nucleus and transverse structure loss)

results thus indicated the differentiated effect of co-treatment formulation on DOX-induced cardiotoxicity and the effectiveness of CPMDC that could nearly bring the two major physiological indices back to normal.

In order to quantitatively evaluate the protective efficacy of CPMSD against cardiotoxic side effects caused by DOX dosing, biochemical analysis was further performed on the crucial markers involved in cardiac toxicity, including SOD and MDA in heart tissues, and LDH, CK, and cTnT in plasma (Ewer and Ewer 2010; Zhang et al. 2018). When compared with the NC group, the mice administered free DOX alone showed significantly decreased SOD level along with elevated MDA content ($p < 0.01$), suggesting the DOX-induced oxidative injury and remarkable amelioration of co-administration of SAA through the CPMDC formulation (Fig. 9B). Meanwhile, significant increases in plasma level of LDH, CK, and cTnT could correspondingly be observed in the mice administered free DOX alone or the simple cocktail of DOX and SAA (Fig. 9C), which confirmed the occurrence of cardiac injury in both DOX and cocktail group. Comparison among these DOX-containing formulations further revealed the reducing effect on all these markers of co-treatment with SAA by CPMDC, but not the cocktail of free DOX and SAA ($p < 0.01$). Due to the effective protection against DOX-induced cardiotoxicity, it therefore was concluded that the tumor-bearing mice would greatly benefit from the present CPMSD formulation of DOX and SAA into dual drug-loaded polymeric micelles.

Finally, the histopathological examination of cardiac tissue specimens was performed to manifest DOX-induced toxic injuries on the main target organ. As illustrated in Fig. 9D, the tumor-bearing nude mice in NC group showed basically normal morphology of cardiac myocyte in the left ventricle, while the DOX-containing treatments could affect cardiomyocytes in different ways and to different degrees depending on the formulation, among which the severest myocardial damage was observed in the mice only treated with free DOX. Accompanied by infiltration of inflammatory cells, the DOX alone group exhibited obvious myocardial injuries, such as cross-striations, myocardial endochylema puffing, and sarcoplasmic matrix partly resorbed, as well as myocardial fiber disarrangement, cellular swelling, and degeneration, hinting toward toxin-mediated necrosis of cardiomyocytes. More to the point, these DOX-induced cardiomyocytes injuries could be alleviated by co-administering SAA, especially through the CPMSD micelles, which displayed less histopathological changes than the cocktail formulation at an equivalent dosage. These findings altogether demonstrated the high potency of SAA against cardiotoxic effect of DOX by co-administering both drugs through the CPMSD formulation.

Conclusions

The present study was an important part of finding efficient strategies for high-performance chemotherapy of breast cancer. By using biocompatible copolymer carrier, CPMSD was developed as an advanced multifunctional polymeric micellar delivery system co-loading the anticancer drug DOX and potent natural antioxidant SAA to overcome the dose-dependent cardiotoxicity associated with cancer therapy**.** Based on optimal formulation, the complex polymeric micelles CPMSD could be constructed by colloidal self-assembly of the amphiphilic copolymer of mPEG-PCL, which integrated

SAA into the hydrophobic cavity and bound DOX to the ball-shaped surface. CPMSD was demonstrated to have favorable physico-pharmaceutical properties, as well as the specific effect of killing two birds with one stone by maintaining the anticancer efficacy of DOX against the associated cardiotoxicity, which thus provide it a great promise for clinical translation as an improved nano-formulation of the well-known anticancer drug. Further investigations would be focused on drug–drug interactions that play a pivotal role in combination therapy.

Abbreviations

DOX	Doxorubicin
SAA	Salvianolic acid A
IARC	International Agency for Research on Cancer
WHO	World Health Organization
TNBC	Triple-negative breast cancer
FDA	Food and Drug Administration
ROS	Reactive oxygen species
PMs	Polymeric micelles
CPMSD	Compound micelles of DOX and SAA
PBS	Phosphate-buffered solution
PDI	Polydispersity index
DLC	Drug loading content
EE	Entrapment efficiency
DOE	Design of experiment
BBD	Behnken design
MM	Molecular mechanics
MD	Molecular dynamics
CLSM	Confocal laser scanning microscopy
ESI	Electrospray ionization
MRM	Multiple reaction monitoring
LDH	Lactate dehydrogenase
CK	Creatine kinase
cTnT	Cardiac troponin T
MDA	Malondialdehyde
SOD	Superoxide dismutase
PLA	Polylactide
PCL	Polycaprolactone
EPR	Enhanced permeability and retention
MPS	Mononuclear phagocyte system
RES	Reticuloendothelial system
KPI	Key performance indices
IC50	Half inhibitory concentration
NC	Negative control
TGI	Tumor growth inhibition

Supplementary Information

The online version contains supplementary material available at https://doi.org/10.1186/s12645-022-00127-w.

Additional file 1: Table S1. Freeze–drying process setup conditions. **Figure S1.** Micellar freeze–drying temperature curve.

Acknowledgements
Not applicable.

Author contributions
ZL, HX, and HW contributed to conceptualization and supervision; ZL, JL, and ZS were involved in data curation; ZL and JL performed formal analysis; HX and HW contributed to funding acquisition; HX supervised investigation; ZL, ZS, and YL contributed to methodology; HX, HW, and FZ performed project administration; ZS and BY provided software; HX and YL did validation; HX, ZL, and ZS contributed to visualization; ZL and JL wrote original draft; HX and FZ were involved in writing—review and editing. All authors have agreed to the published version of the manuscript. All authors read and approved the final manuscript.

Funding
This work was supported by the National Natural Science Foundation of China (82073888), Science and Technology Support Program for Youth Innovation in Universities of Shandong (2019KJM009), Natural Science Foundation of Shandong

Province (No. ZR2019MB054), Science and Technology Project of TCM in Shandong Province (Nos. 2020Z37, 2020M190), Graduate Innovation Foundation of Yantai University (GIFYTU No. YDZD2031), the Top Talents Program for One Case Discussion of Shandong Province, China, Natural Science Foundation of Shandong Province (ZR2021LSW011), and Bohai rim Advanced Research Institute for Drug Discovery (No. LX211011).

Availability of data and materials
The datasets used and analyzed during the current study are available from the corresponding author on reasonable request.

Declarations

Ethics approval and consent to participate
All animal experimental procedures were conducted by following the National Institutes of Health (NIH) guidelines and approved by the Animal Experimentation Ethics Committee of Yantai University, China.

Consent for publication
All authors agree to publish this manuscript in this journal.

Competing interests
The author reports no conflicts of interest in this work.

Received: 13 February 2022 Accepted: 20 June 2022
Published online: 04 July 2022

References

Benzer F, Kandemir FM, Ozkaraca M, Kucukler S, Caglayan C (2018) Curcumin ameliorates doxorubicin-induced cardiotoxicity by abrogation of inflammation, apoptosis, oxidative DNA damage, and protein oxidation in rats. J Biochem Mol Toxicol 32:e22030

Blum JL, Flynn PJ, Yothers G et al (2017) Anthracyclines in early breast cancer: the ABC Trials-USOR 06-090, NSABP B-46-I/USOR 07132, and NSABP B-49 (NRG oncology). J Clin Oncol 35(23):2647–2655

Bray F, Ferlay J, Soerjomataram I, Siegel RL, Torre LA, Jemal A (2018) Global cancer statistics 2018: GLOBOCAN estimates of incidence and mortality worldwide for 36 cancers in 185 countries. CA Cancer J Clin 68:394–424

Chatterjee K, Zhang J, Honbo N, Karliner JS (2010) Doxorubicin cardiomyopathy. Cardiology 115(2):155–162

Chegaev K, Riganti C, Rolando B et al (2013) Doxorubicin-antioxidant co-drugs. Bioorg Med Chem Lett 23(19):5307–5310

Cvetković RS, Scott LJ (2005) Dexrazoxane: a review of its use for cardioprotection during anthracycline chemotherapy. Drugs 65(7):1005–1024

Duggan ST, Keating GM (2011) Pegylated liposomal doxorubicin. A review of its use in metastatic breast cancer, ovarian cancer, multiple myeloma and AIDS-related Kaposi's sarcoma. Drugs 71(18):2531–2558

Ewer MS, Ewer SM (2010) Cardiotoxicity of anticancer treatments: what the cardiologist needs to know. Nat Rev Cardiol 7(10):564–575

Fan HY, Yang L, Fu FH et al (2012) Cardioprotective effects of salvianolic acid A on myocardial ischemia-reperfusion injury in vivo and in vitro. Evid Based Complement Altern Med. https://doi.org/10.1155/2012/508938

Fan HY, Yang MY, Qi D et al (2015) Salvianolic acid A as a multifunctional agent ameliorates doxorubicin-induced nephropathy in rats. Sci Rep 5:12273

Foloppe N, MacKerell A (2000) All-atom empirical force field for nucleic acids: I. Parameter optimization based on small molecule and condensed phase macromolecular target data. J Comput Chem 21:86–104

Gong C, Deng S, Wu Q et al (2013) Improving antiangiogenesis and anti-tumor activity of curcumin by biodegradable polymeric micelles. Biomaterials 34(4):1413–1432

Guo Z, Yan M, Chen L et al (2018) Nrf2-dependent antioxidant response mediated the protective effect of tanshinone IIA on doxorubicin-induced cardiotoxicity. Exp Ther Med 16:3333–3344

Hou YY, Peng JM, Chao RB (2007) Pharmacokinetic study of salvianolic acid A in rat after intravenous administration of Danshen injection. Biomed Chromatogr 21:598–601

Hou B, Qiang G, Zhao Y et al (2017) Salvianolic acid A protects against diabetic nephropathy through ameliorating glomerular endothelial dysfunction via inhibiting AGE-RAGE signaling. Cell Physiol Biochem 44(6):2378–2394

Jiang YX, Wang F, Xu H, Liu H, Meng QG, Liu WH (2014) Development of andrographolide loaded PLGA microspheres: optimization, characterization and in vitro–in vivo correlation. Int J Pharm 475(1–2):475–484

Jorgensen WL, Maxwell DS, Tirado-Rives J (1996) Development and testing of the OPLS all-atom force field on conformational energetics and properties of organic liquids. J Am Chem Soc 118(45):11225–11236

Kaiserova H, Simunek T, van der Vijgh WJ, Aalt B, Kvasnickova E (2007) Flavonoids as protectors against doxorubicin cardiotoxicity role of iron chelation, antioxidant activity and inhibition of carbonyl reductase. BBA-Mol Basis Dis 1772(9):1065–1074

Kane RC, Mcguinn WD, Dagher R, Justice R, Pazdur R (2008) Dexrazoxane (Totect™): FDA review and approval for the treatment of accidental extravasation following intravenous anthracycline chemotherapy. Oncologist 13(4):445–450

Kuerban K, Gao X, Zhang H, Liu J, Dong M, Wu L, Ye R, Feng M, Ye L (2020) Doxorubicin-loaded bacterial outer-membrane vesicles exert enhanced anti-tumor efficacy in non-small-cell lung cancer. Acta Pharm Sin B 10(8):1534–1548

Kwon GS, Kataoka K (2012) Block copolymer micelles as longcirculating drug vehicles. Adv Drug Del Rev 64(2–3):237–245

Li X, Wu XH, Yang HY, Li L, Ye ZQ, Rao YF (2019) A nuclear targeted Dox-aptamer loaded liposome delivery platform for the circumvention of drug resistance in breast cancer. Biomed Pharmacother 117:109072

Li FF, Liu ZL, Sun HY et al (2020a) PCC0208017, a novel small-molecule inhibitor of MARK3/MARK4, suppresses glioma progression in vitro and in vivo. Acta Pharm Sin B 10(2):289–300
Li Z, Xiao C, Yong TY, Li ZF, Gan L, Yang XL (2020b) Influence of nanomedicine mechanical properties on tumor targeting delivery. Chem Soc Rev 49(8):2273–2290
Lin TJ, Liu GT, Liu Y, Xu GZ (1992) Protection by salvianolic acid A against adriamycin toxicity on rat heart mitochondria. Free Radic Biol Med 12(5):347–351
Liu H, Xu H, Jiang Y et al (2015) Preparation, characterization, in vivo pharmacokinetics, and biodistribution of polymeric micellar dimethoxycurcumin for tumor targeting. Int J Nanomed 10:6395–6410
Ma Z, Li N, Zhang B et al (2020) Dual drug-loaded nano-platform for targeted cancer therapy: toward clinical therapeutic efficacy of multifunctionality. J Nanobiotechnol 18(1):123
Mitry MA, Edwards JG (2016) Doxorubicin induced heart failure: phenotype and molecular mechanisms. Int J Cardiol Heart Vasc 10:17–24
Moore TL, Rodriguez-Lorenzo L, Hirsch V et al (2015) Nanoparticle colloidal stability in cell culture media and impact on cellular interactions. Chem Soc Rev 44(17):6287–6305
Pei LX, Bao YW, Wang HD et al (2008) A sensitive method for determination of salvianolic acid A in rat plasma using liquid chromatography tandem mass spectrometry. Biomed Chromatogr 22:786–794
Shaikh F, Dupuis LL, Alexander S, Gupta A, Mertens L, Nathan PC (2016) Cardioprotection and second malignant neoplasms associated with dexrazoxane in children receiving anthracycline chemotherapy: a systematic review and meta-analysis. J Natl Cancer Inst 4:46–69
Shen Y, Wang XY, Xu LH, Liu XW, Chao RB (2009) Characterization of metabolites in rat plasma after intravenous administration of salvianolic acid A by liquid chromatography/time of-flight mass spectrometry and liquid chromatography/ion trap mass spectrometry. Rapid Commun Mass Spectrom 23(12):1810–1816
Sinha VR, Bansal K, Kaushik R et al (2004) Polyepsilon-caprolactone microspheres and nanospheres: an overview. Int J Pharm 278(1):1–23
Spalatoceruso M, Napolitano A, Silletta M et al (2019) Use of cardioprotective dexrazoxane is associated with increased myelotoxicity in anthracycline-treated soft-tissue sarcoma patients. Chemotherapy 64(2):1–5
Sun GB, Wang J, Zhang MD, Sun XB (2017) Salvianolic acid B attenuates doxorubicin-induced ER stress by inhibiting TRPC3 and TRPC6 mediated Ca2+ overload in rat cardiomyocytes. Tocical Lett 276:21–30
Szaflarski W, Sujka-Kordowska P, Januchowski R et al (2013) Nuclear localization of P-glycoprotein is responsible for protection of the nucleus from doxorubicin in the resistant LoVo cell line. Biomed Pharmacother 67(6):497–502
Torchilin VP (2007) Micellar nanocarriers: pharmaceutical perspectives. Pharm Res 24(1):1–16
Tsou SH, Chen TM, Hsiao HT, Chen YH (2015) A critical dose of doxorubicin is required to alter the gene expression profiles in MCF-7 cells acquiring multidrug resistance. PLoS ONE 10(1):e0116747
Waks AG, Winer EP (2019) Breast cancer treatment: a review. JAMA 321:288–300
Wei W, Li S, Xu H et al (2018) MPEG-PCL copolymeric micelles for encapsulation of azithromycin. AAPS PharmSciTech 19(5):2041–2047
Wicki A, Witzigmann D, Balasubramanian V, Huwyler J (2015) Nanomedicine in cancer therapy: challenges, opportunities, and clinical applications. J Control Release 200:138–157
Xu H, Li YL, Che X et al (2014) Metabolism of salvianolic acid A and antioxidant activities of its methylated metabolites. Drug Metab Dispos 42(2):274–281
Yin QK, Liu XC, Hu L et al (2021) VE-822, a novel DNA Holliday junction stabilizer, inhibits homologous recombination repair and triggers DNA damage response in osteogenic sarcomas. Biochem Pharmacol 93:114767
Yu J, Wang Y, Zhou S, Li J, Wang J, Chi D, Wang X, Lin G, He Z, Wang Y (2020) Remote loading paclitaxel-doxorubicin prodrug into liposomes for cancer combination therapy. Acta Pharm Sin B 10(9):1730–1740
Zhai Y, Zhou X, Jia L et al (2017) Acetal-linked paclitaxel polymeric prodrug based on functionalized mPEG-PCL diblock polymer for pH-triggered drug delivery. Polymers 119(12):698
Zhang D, Xu Q, Wang N et al (2018) A complex micellar system co-delivering curcumin with doxorubicin against cardiotoxicity and tumor growth. Int J Nanomed 13:4549–4561
Zhang JW, Yu GH, Yang YT et al (2022) A small-molecule inhibitor of MDMX suppresses cervical cancer cells via the inhibition of E6-E6AP-p53 axis. Pharmacol Res 177:106128
Zhou L, Zuo Z, Chow MS (2013) Danshen: an overview of its chemistry, pharmacology, pharmacokinetics, and clinical use. J Clin Pharmacol 53(12):787–811
Zuo JX, Jiang YM, Zhang EX et al (2019) Synergistic effects of 7-*O*-geranylquercetin and siRNAs on the treatment of human breast cancer. Life Sci 227:145–152

Publisher's Note